Importance of a stochastic distribution of floods and erosion thresholds in the bedrock river incision problem

Noah P. Snyder[1] and Kelin X. Whipple

Department of Earth, Atmospheric and Planetary Sciences, Massachusetts Institute of Technology, Cambridge, Massachusetts, USA

Gregory E. Tucker

School of Geography and the Environment, University of Oxford, Oxford, UK

Dorothy J. Merritts

Geosciences Department, Franklin and Marshall College, Lancaster, Pennsylvania, USA

[1] Fluvial erosion of bedrock occurs during occasional flood events when boundary shear stress exceeds a critical threshold to initiate incision. Therefore efforts to model the evolution of topography over long timescales should include an erosion threshold and should be driven by a stochastic distribution of erosive events. However, most bedrock incision models ignore the threshold as a second-order detail. In addition, climate is poorly represented in most landscape evolution models, so the quantitative relationship between erosion rate and measurable climatic variables has been elusive. Here we show that the presence of an erosion threshold, when combined with a well-constrained, probabilistic model of storm and flood occurrence, has first-order implications for the dynamics of river incision in tectonically active areas. First, we make a direct calculation of the critical shear stress required to pluck bedrock blocks for a field site in New York. Second, we apply a recently proposed stochastic, threshold, bedrock incision model to a series of streams in California, with known tectonic and climatic forcing. Previous work in the area has identified a weak relationship between channel gradient or relief and rock uplift rate that is not easily explained by simpler detachment-limited models. The results with the stochastic threshold model show that even low erosion thresholds, which are exceeded in steep channels during high-frequency flood events, fundamentally affect the predicted relationship between gradient and uplift rate in steady state rivers, in a manner consistent with the observed topography. This correspondence between theory and data is, however, nonunique; models in which a thin alluvial cover may act to inhibit channel incision in the low uplift rate zone also provide plausible explanations for the observed topography. Third, we explore the broader implications of the stochastic threshold model to the development of fluvial topography in active tectonic settings. We suggest that continued field applications of geomorphic models, including physically meaningful thresholds and stochastic climate distributions, are required to advance our knowledge of interactions among surficial, climatic, and crustal processes.   *INDEX TERMS:* 1815 Hydrology: Erosion and sedimentation; 1824 Hydrology: Geomorphology (1625); 1869 Hydrology: Stochastic processes; 8107 Tectonophysics: Continental neotectonics; *KEYWORDS:* tectonic geomorphology, erosion, bedrock channels, relief, thresholds, stochastic processes

1. Introduction

[2] Numerous recent field, laboratory, and modeling efforts have been devoted to understanding rates and

processes of bedrock-river incision [*Howard and Kerby*, 1983; *Willgoose et al.*, 1991; *Sklar and Dietrich*, 1998; *Tinkler and Wohl*, 1998; *Stock and Montgomery*, 1999; *Snyder et al.*, 2000; *Whipple et al.*, 2000a], with the goal of understanding the evolution of topography in response to tectonic and climatic forcings. At a fundamental level, all research efforts indicate that bedrock incision rate is set by channel gradient, among other factors. Much debate centers on the exact nature of the quantitative relationship

[1]Now at U.S. Geological Survey Pacific Science Center, Santa Cruz, California, USA.

between gradient and incision rate, and the relative importance of channel width, substrate lithology and sediment flux. At steady state (rock uplift rate balanced by incision rate), in general, steeper channels correlate with higher uplift rates. Moreover, because channel gradient sets drainage basin topographic relief, steady state fluvial relief correlates positively with uplift rate [e.g., *Whipple and Tucker*, 1999]. Therefore well-constrained bedrock incision models will allow us to make predictions and test hypotheses about the development of relief in tectonically active areas.

[3] Models based on bed shear stress [*Howard and Kerby*, 1983; *Willgoose et al.*, 1991; *Stock and Montgomery*, 1999; *Snyder et al.*, 2000] typically have made the simplifying assumption (either explicitly or implicitly) that bedrock erosion occurs during major flood events [*Baker and Kale*, 1998] when boundary shear stress is far greater than the threshold value necessary to initiate incision, and that therefore the threshold term can be neglected. However, a recent analysis using stochastic, threshold erosion theory [*Tucker and Bras*, 2000] reveals that this assumption leads to physically unrealistic behavior, with the least variable climate producing the highest erosion rates. This runs counter to the assumption used to justify ignoring the threshold term, and counter to the hypothesis that erosion is more efficient in stormier climates [*Molnar and England*, 1990; *Bull*, 1991; *Peizhen et al.*, 2001]. Motivated by this observation, here we (1) make a direct estimate of the critical shear stress required to initiate incision by joint block plucking on the bed of a river in New York and (2) investigate the implications of the Tucker and Bras model [*Tucker and Bras*, 2000; G.E. Tucker, Drainage basin sensitivity to tectonic and climatic forcing: Implications of a stochastic model for the role of entrainment and erosion thresholds, *Earth Surface Processes and Landforms*, submitted, 2002, hereinafter referred to as Tucker, submitted manuscript, 2002] for the development of topography in orogenic settings, including an application of the model to a well-constrained field location in northern California [*Merritts and Bull*, 1989; *Merritts and Vincent*, 1989; *Snyder et al.*, 2000, 2003]. Inclusion of these two approaches highlights the importance of thresholds in fluvial erosion, at the level of individual floods and as part of a distribution of events. Here we extend the analysis of *Tucker and Bras* [2000] to elucidate broader tectonic implications of the stochastic threshold model, with emphasis on the relationship between steady state fluvial relief and rock uplift rate. These model predictions are supported by data from the California study. This correspondence is nonunique, however, and other explanations of the observed relief contrast are discussed. We also investigate the theoretical implications of the stochastic threshold model to settings with spatially variable rock uplift rate [*Kirby and Whipple*, 2001]. Through application of surface process models to well-constrained field settings, we can begin to bridge the gap between our understanding of erosion driven by individual floods (e.g., our analysis in New York) that are part of a stochastic distribution of events [*Benda and Dunne*, 1997], and our understanding of erosion rates over geologic timescales (e.g., our analysis in California) that are

central to efforts to model crustal and atmospheric interactions [*Willet*, 1999].

2. Threshold Shear Stress For Plucking

[4] Many workers [e.g., *Howard and Kerby*, 1983; *Howard et al.*, 1994; *Whipple and Tucker*, 1999] have postulated that bedrock-river incision rate (E) is a power law function of boundary shear stress (τ_b) above a threshold (or critical) shear stress (τ_c):

$$E = k_e(\tau_b - \tau_c)^a \tag{1a}$$

or

$$E = k_e(\tau_b^a - \tau_c^a)^a \tag{1b}$$

where k_e is a coefficient of erosion dependent on lithologic resistance and erosion process and a is an exponent dependent on erosion process. Equation (1a) is the commonly used "excess shear stress" form. Equation (1b) is similar, equally defensible, and more tractable in some applications (Tucker, submitted manuscript, 2002).

[5] In the case where incision rates are set by plucking of intact blocks along joint or fracture planes, *Whipple et al.* [2000a] argued that the value of a in equation (1) should be unity, or slightly higher. In their treatment, other hypothesized incision processes (abrasion, cavitation) likely have higher values of a. Here, we consider values of a from 1 to 10/7, consistent with field observations that plucking (in the sense defined by *Whipple et al.* [2000a]) is the dominant process in the rivers studied. This situation applies to areas with rocks that are sufficiently fractured to allow fluvial transport of exposed blocks, particularly appropriate when bedrock either (1) is highly fractured (joint spacing 0.1 to 1 m), or (2) breaks into blocks with a small height-to-length ratio [*Whipple et al.*, 2000a]. Importantly, most previous analyses of incision by plucking processes have acknowledged or even emphasized the importance of τ_c [e.g., *Baker and Kale*, 1998; *Hancock et al.*, 1998; *Howard*, 1998; *Whipple et al.*, 2000a]. One limitation of the approach in equation (1) is that it does not take into account the role that sediment flux and sediment supply (with associated stochastic distributions and transport threshold) might play in driving incision of bedrock [*Howard*, 1980; *Beaumont et al.*, 1992; *Sklar and Dietrich*, 1998; *Whipple and Tucker*, 2002].

[6] The threshold term (τ_c) must, at a minimum, equal the shear stress necessary to transport coarse bedload in a given river system. Bedload transport is known to be a threshold-dependent process [e.g., *Gomez and Church*, 1989; *Buffington and Montgomery*, 1997], and if it is not in motion, the bed material will protect the channel floor from erosion [*Sklar and Dietrich*, 1998; *Whipple and Tucker*, 2002]. In settings with resistant bedrock, τ_c may be set by the properties of substrate lithology, in this case the threshold for incision likely exceeds the τ_c appropriate for sediment transport.

[7] Boundary shear stress (τ_b) can be estimated from field data. Assuming steady, uniform flow, τ_b is approximated by the product of depth (d) and slope (S):
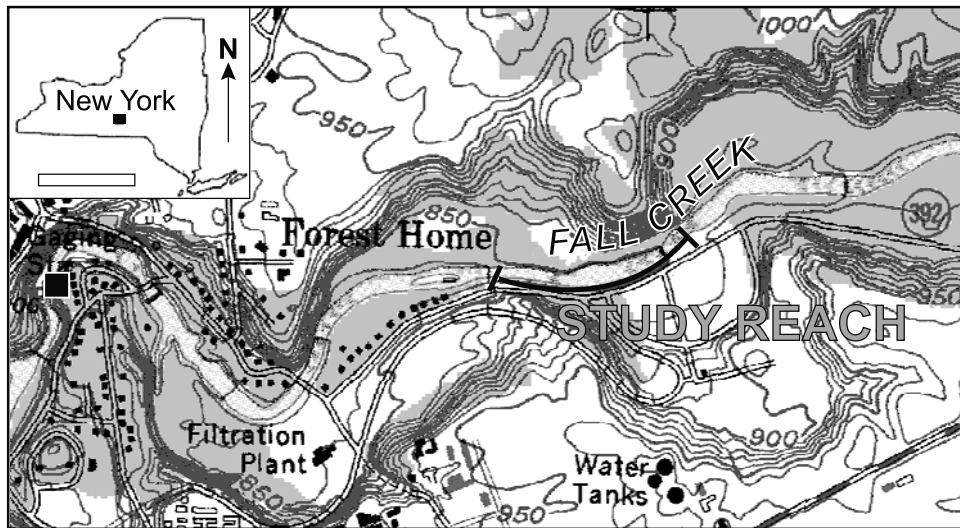
$$\tau_b = \rho g d S, \tag{2}$$

Figure 1. Location map for Flat Rock, Fall Creek study area. Base is the U.S. Geological Survey 7.5'
Ithaca East, New York quadrangle, contour interval 10 feet (1 foot = 0.3 m). USGS stream-gaging station
used in this study is indicated by the black box on the west side of the map, ~1 km downstream of the
study reach. Inset map indicates position within New York state; bar represents 200 m of distance on the
study area map.

where ρ is the density of water and g is gravitational
acceleration. Combining equation (2) with the Manning
friction relationship gives

$$\tau_b = \rho g N^{3/5} \left(\frac{Q}{w}\right)^{3/5} S^{7/10}, \qquad (3)$$

where Q is discharge, w is channel width, and N is the
Manning roughness coefficient. The value of τ_b given by
equations (2) and (3) is the total boundary shear stress,
including both skin friction and momentum losses due to
form drag on bed or bank roughness elements. For the
motion of large blocks, this inclusion of form drag
components is appropriate as the blocks themselves largely
determine boundary roughness. The parameters in equations
(2) and (3) needed to estimate τ_b can be measured from field
and hydrologic data.

[8] In contrast to τ_b, threshold shear stress (τ_c) is difficult
to evaluate from field or experimental data. We are aware of
no previous studies that actually calculate τ_c for bedrock
incision, although measurements of τ_b clearly in excess of
τ_c have been made for large paleofloods [*Baker and Kale*,
1998]. Numerous workers (see review by *Buffington and
Montgomery* [1997]) have studied the threshold for particle
motion in alluvial bed rivers, but these calculations are only
relevant to this of study bedrock channels in that they
provide minimum estimates of τ_c. The case of sediment
mobilization on a noncohesive bed of similar sized particles
is quite different from the plucking of large joint blocks.
Here we present two calculations of τ_c for incision of
bedrock. First, we apply field data from a 1981 flood event
in New York to equations (2) and (3) to get an estimate of
total boundary shear stress during an observed plucking
event. Second, we use data from a well-constrained field
site in northern California to back calculate the critical shear
stress that best models an observed relationship between
channel gradient (and therefore topographic relief) and rock
uplift rate [*Snyder et al.*, 2000, 2003]. Because the method-

ologies, timescales, and geologic settings of these two
examples are entirely different, these calculations are not
comparable to one another, but both demonstrate the
importance of erosion thresholds.

3. Estimation of Critical Shear Stress at Fall Creek, Ithaca, New York

3.1. Setting

[9] Fall Creek is major west flowing tributary of Cayuga
Lake at Ithaca, in the Finger Lakes region of central New
York in the United States. The southern lobes of Lake
Ontario ice caps covered the region, and scoured out and
oversteepened the lake basins [*Mullins et al.*, 1996]. Upper
Fall Creek flows through a valley formerly occupied by a
Wisconsinan ice tongue. The retreating glacier left the valley
filled with at least 35 m of poorly sorted sand and gravel
overlain by till. The creek is actively incising through this
fill. Near the Cornell University campus, Fall Creek enters a
steep bedrock gorge and drops about 200 m over several
waterfalls before entering the southern end of Cayuga Lake.

[10] The study site (Figure 1), locally known as "Flat
Rock," is the farthest upstream section of bedrock-floored
channel in Fall Creek, where the river is superposed on a
bedrock rib. This rock is much less erodible than the glacial
deposits upstream, and the site therefore dictates the base
level for the rest of the creek (a drainage area of 326 km²).
During the time since deglaciation (no more than 14 kyr
[*Mullins et al.*, 1996]), ~2 vertical meters of bedrock have
been eroded at Flat Rock, judging from strath terrace
exposures. The 500-m study reach is located immediately
downstream from a 1.5-m-high weir that is the water supply
intake point for Cornell University. The weir marks the
uppermost exposed bedrock in Fall Creek.

3.2. Lithology

[11] The study reach is underlain by the Upper Devon-
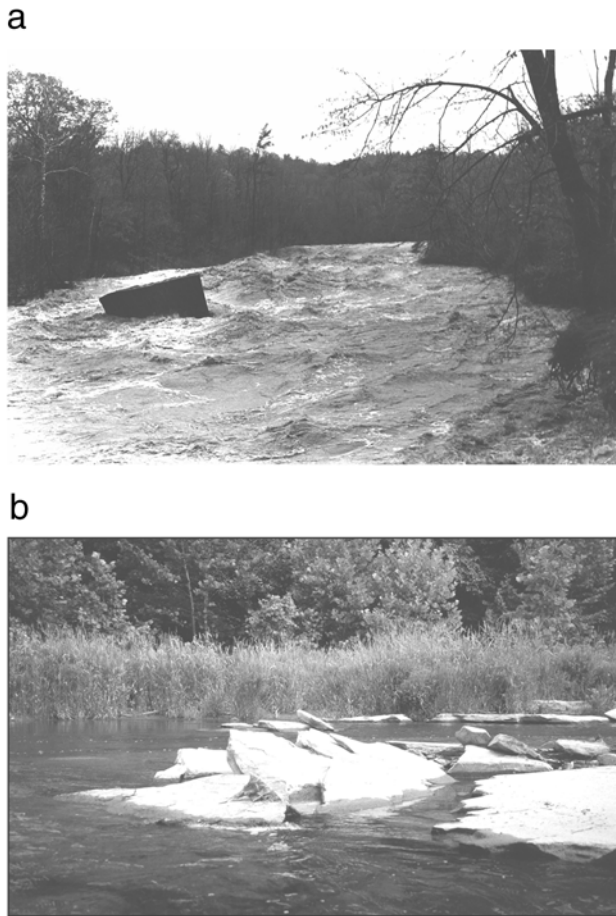ian Ithaca Formation of shale, siltstone and thin-bedded

Figure 2. Photographs of the Fall Creek study area. (a) A view east from the downstream end of the field area of a large plucked block (~4 m in length) actively tumbling downstream at Flat Rock, during the 28 October 1981 flood. Channel width here is 25–52 m (Table 1a). Photograph by R. Palmer. (b) Imbricated blocks at Flat Rock during postflood, low-flow conditions.

(1–30 cm) sandstone. The rock is cut by multiple sets of vertical joints spaced 1–4 m apart. Schmidt hammer measurements on exposed joint planes yield a mean rock mass strength of 51.7 ± 6.8 R units (1σ, n = 25); and measurements on subhorizontal bedding planes give 46.4 ± 8.5 R (n = 70). For information on the Schmidt hammer methodology used here, see *Snyder et al.* [2003].

3.3. The 28 October 1981 Flood Event

[12] Plucking of large bedrock slabs (up to 4 m long × 2 m wide × 30 cm thick) from in-place positions on the river bed occurred at Flat Rock during a major flood event on 28 October 1981 (Figure 2). The flood was the result of 2.6 cm of rain on 27 October and 12.9 cm on 28 October, a 2-day storm total well above the October monthly mean precipitation of 8.3 cm (Cornell University, Ithaca, New York, station data from the Northeast Regional Climate Center). The peak discharge (Q_{pk}) measured at the Fall Creek (Ithaca) gauging station ~1 km downstream of the study reach (Figure 1) was 335 m³ s⁻¹. This event was the second largest in the 75-year record at

this station (Q_{pk} = 439 m³ s⁻¹ on 8 July 1935). The 1981 event was the only flood that caused significant plucking of large blocks at Flat Rock in at least the past ~40 years, as deduced from visual observations during annual visits to the site with an undergraduate geomorphology class throughout this period (A. L. Bloom, personal communication, 2000). It significantly modified the morphology of Flat Rock, a popular swimming spot, and washed out several bridges upstream.

3.4. Dominant Erosion Process

[13] We infer that plucking of bedding plane blocks is the important incision process in this location. Less dramatic erosion of bedrock, such as abrasive rounding of block corners, likely occurs frequently during smaller flood events. However, this is the result of a fundamentally different process than plucking of the large blocks that characterize the bed. Interflood processes are undoubtedly important in preparing large blocks for plucking. The existence of a critical threshold for plucking of bedrock blocks has been argued by numerous workers [e.g., *Baker and Kale*, 1998; *Hancock et al.*, 1998; *Howard*, 1998; *Whipple et al.*, 2000a]. The low erosion rate in the field setting (only ~2 m in ~14 kyr) further argues that events capable of removing blocks 30-cm-thick from any given point on the bed are rare, although several such events would be required to lower the entire bed 30 cm. We cannot rule out highly nonlinear erosion processes ($a \gg 1$), but the major modification of the field site that occurred during the 1981 flood, combined with intrinsic properties of the jointed bedrock and theoretical physical considerations, argues that threshold plucking is the rate-limiting process in this field site.

3.5. Methods

[14] We measured channel gradient (S) for the study reach, and estimated the flow depth (d), and channel width (w) that occurred during the 1981 flood (Table 1). The latter two were obtained using field measurements at four representative locations along the 0.5-km study reach. We used reference marks on photographs of the event (Figure 2a) to estimate flow conditions during the flood. Depth (d) and width (w) were measured using a stadia rod and hand level (± 20 cm), and laser range finder (± 1 m), respectively. Because the channel bank on the north side has a series of terraces cut in glacial sediments, we made two estimates of w: high flow (to edge of the first north bank terrace) and valley width (the maximum width possible during the flood, based on photographs). Because S was the parameter most difficult to measure with precision, we used three approximations of local water surface slope during the event, all based on the bed slope. The first two (mean slope over the 0.5-km study reach and over the 100-m reach surrounding each width measurement station) were from a hand level and stadia rod field survey of the channel bed, with 10-m horizontal spacing. The third slope measurement was from the USGS 7.5' Ithaca East quadrangle map. This estimate includes the ~1.5 m drop of the weir and is therefore a maximum estimate of the relevant slope over the reach. Finally, Manning's roughness coefficient (N) was estimated by

Table 1a. Total Boundary Shear Stress (τ_b) Estimates for Each Measurement Station[a]

Station	Distance From Weir, m	Local Slope S	High-Flow Width w_h, m	Valley Width w_v, m	Flow Depth d, m	τ_b Range, Pa	
						Equation (2)	Equation (3)
1	90	0.0059	25	40	2.4	106–186	132–260
2	180	0.0007	36	41	2.7	19–211	35–209
3	330	0.0032	50	52	2.3	72–178	89–172
4	500	0.0062	32	39	2.3	101–178	134–224

[a]Ranges in τ_b reflect three slope estimates (100-m local survey, reach survey mean, and topographic map measurement; Table 1b) and two width measurements (w_h, w_v).

comparison to similar streams [*Barnes*, 1967; *Coon*, 1998].

3.6. Results and Interpretation

[15] The calculations of boundary shear stress (τ_b) during the 1981 flood event are presented in Table 1. Mean estimates of τ_b for the four stations range from 92 to 188 Pa based on equation (2) and from 123 to 202 Pa based on equation (3) (Table 1b). These ranges reflect the differing slope and width estimates for each station. Because floods of only slightly lower magnitude than the 1981 event apparently failed to initiate plucking, we infer that the critical shear stress (τ_c) for this site is only slightly less than our estimates of τ_b. The range of estimated τ_c values is consistent with *Magilligan*'s [1992] review of thresholds for extreme reworking of channel morphology. In summary, we emphasize that the 1981 flood was a rare, extreme event, consistent with the low postglacial incision rate of the site.

4. A Stochastic Distribution of Floods and Erosion Thresholds in a Bedrock Channel Incision Model

[16] The 1981 Fall Creek flood highlights the importance of large, infrequent events in river incision [*Baker and Kale*, 1998]. Such events can be incorporated into geomorphic models using a realistic frequency distribution of floods, along with a threshold for initiating erosion. We know that bedrock erosion must occur during flood events that are at least capable of transporting coarse bedload, which only occurs in floods that exceed a threshold boundary shear stress [e.g., *Gomez and Church*, 1989; *Buffington and Montgomery*, 1997]. It follows then that bedrock erosion models should include a threshold term at a minimum appropriate to transport coarse bedload. Naturally, the threshold for incision into competent rock will often exceed this initiation of motion threshold. However, modeling approaches based on a single "characteristic" erosive flood (i.e., bankfull), such as those used in our previous works [*Snyder et al.*, 2000, 2003] are fundamentally incompatible

Table 1b. Total Boundary Shear Stress (τ_b) Estimates for Different Slope Measurement Mean Values From Each Station[a]

Slope Measurement	τ_b, Pa	
	Equation (2)	Equation (3)
Map, S = 0.0079	188	202
Survey mean, S = 0.0045	107	137
100-m survey mean (see above)	92	123

[a]$Q = 335$ m^3 s^{-1}; $g = 9.8$ m s^{-2}; $\rho = 1000$ kg m^{-3}; $N = 0.05$ m$^{-1/3}$s.
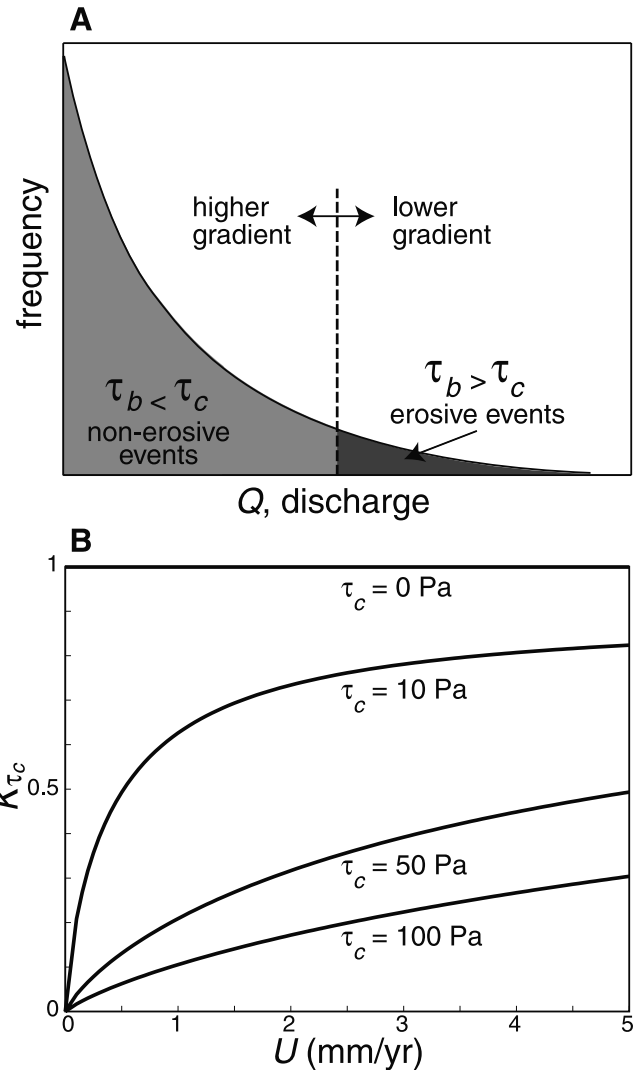

Figure 3. Stochastic threshold model concepts. (a) Schematic plot of flood discharge frequency. A flood of a given magnitude is erosive only if it generates basal shear stresses (τ_b) in excess of the threshold shear stress (τ_c). Only a part of the distribution of flood events at a given location will exceed the erosion threshold, introducing an important nonlinearity into the model. For a given location, the threshold discharge of erosion changes inversely with channel gradient, shifting the frequency of erosive events. Modified from *Baldwin et al.* [2003]. (b) General relationship between $K_{\tau c}$ at steady state and rock uplift rate (U), for various values of threshold shear stress (τ_c). Note that the top line ($K_{\tau c} = 1$) represents the $\tau_c = 0$ case.

Table 2a. Poisson Rectangular Pulse Rainfall Parameters[a]

Station	Years of Data	Mean Storm Precipitation Intensity P, m yr^{-1}	Mean Storm Duration T_r, hours	Mean Interstorm Period T_b, hours	Predicted Annual Precipitation $\langle P \rangle = 0.5(T_r/T_r + T_b)P$, m yr^{-1}	Observed Mean Annual Precipitation P_{ma}, m yr^{-1}
Eureka (LUZ)	1954–1993	7.9	20.7	69.7	0.907	0.833
Honeydew (HUZ)	1985–1986	25.3	13.2	74.5	1.915	1.808

[a]Hourly precipitation is from the National Climatic Data Center.

with placing a realistic, physically meaningful value on the threshold term. We know of no means to arrive at a meaningful estimate of a characteristic discharge event for a bedrock river. Such an event, if it exists, would undoubtedly be a function of lithology and climate. The incompatibility occurs because the magnitude of the characteristic discharge event depends on the value of the threshold term, and vice versa. Although the τ_c term may be determined from field data in some settings (e.g., Fall Creek), such measurements do not provide any means to understand the characteristic discharge event for an area. Put another way, the threshold term dictates the minimum flow required to initiate incision at a given river location, so it is only meaningful if a part of the flood frequency distribution is unable to exceed it (Figure 3a). Therefore modeling efforts must include both a stochastic representation of flood events and a threshold shear stress. Bedrock channel incision models that include a threshold shear stress, but not a stochastic distribution of storm events (as noted by *Snyder et al.* [2003]) are fundamentally oversimplified and unsatisfying because they cannot be constrained from field data.

[17] *Tucker and Bras* [2000] developed a means to incorporate a stochastic distribution of rainfall events into a bedrock channel evolution model based on shear stress or unit stream power. As mentioned above, they demonstrated that the inclusion of the threshold term (or a strongly nonlinear relationship between erosion rate and discharge) is necessary to produce model results consistent with the expected correlation between stormier climates and high erosion rates. Importantly, their model allows for a direct, realistic representation of climate and climate change, which is necessary to begin to test hypothesized relationships between climate and erosion. By applying their model to a real, well-studied landscape, we demonstrate the relevance and predictions of the model to the study of tectonically active regions, and explore, for the first time, the broader

implications of the model to the relationship between tectonics and landscape form.

[18] Here we present a synopsis of the stochastic threshold model (Table 2), starting with a brief review of the simple shear stress bedrock incision model. In a previous study [*Snyder et al.*, 2000] we modeled bedrock incision rate (E) using the basic power law form [*Howard and Kerby*, 1983; *Whipple and Tucker*, 1999]:

$$E = KA^m S^n, \qquad (4)$$

where S is channel gradient, A is drainage area (a proxy for discharge, Q), K is the coefficient of erosion (dependent on a variety of factors including lithology, process, climate and channel width), and the exponents m and n are dependent on hydrology, channel hydraulic geometry, and erosion process. As discussed previously by *Snyder et al.* [2003], the main limitations of this approach are that it (1) assumes that all incision occurs during a single "characteristic" discharge event, included in the parameter K; (2) assumes that τ_c is negligible ($\tau_b \gg \tau_c$) during this event; and (3) allows for only a crude inclusion of climatic conditions. Nonetheless, this simple form of the shear stress model does provide a useful framework from which to investigate the bedrock river incision process.

[19] In the case of steady state incision, rock uplift rate (U) can be substituted for incision rate (E), and equation (4) can be solved for steady state slope (S_e):

$$S_e = \left(\frac{U}{K}\right)^{1/n} A^{-m/n}. \qquad (5)$$

This is similar in form to the commonly observed empirical relationship between slope and area [e.g., *Hack*, 1957]:

$$S = k_s A^{-\theta}, \qquad (6)$$

where k_s is the channel steepness index and θ is the channel concavity index. Equations (5) and (6) are equivalent under

Table 2b. Results of Mendocino Triple Junction Streams Calculations[a]

Case	Shear Stress Exponent a	Area Exponent $m = 3/5a(1-b)$	Slope Exponent $n = 7/10a$	Best Critical Shear Stress τ_c[b](Range), Pa	Best Shear Stress Coefficient k_e (Range), Pa^{-a} myr^{-1}
Eureka	1	0.36	0.70	152 (99–218)	1.9 (0.30–29) × 10^{-3}
Eureka (LUZ)-Honeydew (HUZ)	1	0.36	0.70	105 (68–136)	3.6 (1.4–6.0) × 10^{-4}
Eureka	1.43	0.51	1	150 (93–218)	1.3 (0.23–19 × 10^{-4}
Eureka (LUZ)-Honeydew (HUZ)	1.43	0.51	1	95 (45–131)	2.4 (0.94–4.0) × 10^{-5}

[a]See Appendix A for equations. Parameter values are $\rho = 1000$ kg m^{-3}; $g = 9.8$ m s^{-2}; $N = 0.07$ m$^{-1/3}$s; $A_{ref} = 10^6$ m^2; $m/n = 0.514$. Other values are $b = 0.4$ (downstream width discharge exponent [from *Snyder et al.*, 2003]); $s = 0.25$ (at a station width discharge exponent [from *Leopold and Maddock*, 1953]); at LUZ, $U_1 = 0.0005$ m yr^{-1} (0.0003–0.0005 m yr^{-1} [*Merritts and Bull*, 1989; *Merritts*, 1996]); $k_{s1} = 170$ m$^{1.03}$; at HUZ, $U_2 = 0.004$ m yr^{-1} (0.0025–0.004 m yr^{-1}); $k_{s2} = 295$ m$^{1.03}$ (237–388 m$^{1.03}$ [*Snyder et al.*, 2000]); Eureka/LUZ parameters (for 17 February 1975 representative bankfull flood event [from *Snyder et al.*, 2003]) are $k_{q1} = 1.47 \times 10^{-6}$ m s^{-1} (linear discharge area coefficient, $Q = k_q A$) and $k_{w1} = 4.63$ m$^{-0.2}$s$^{0.4}$ (downstream width discharge coefficient, $w = k_w Q^b$); Honeydew/HUZ parameters (for 17 February 1975 representative bankfull flood event [from *Snyder et al.*, 2003]) are $k_{q2} = 2.73 \times 10^{-6}$ m s^{-1}; $k_{w2} = 3.61$ m$^{-0.2}$ s$^{0.4}$.
[b]Critical shear stresses (τ_c) of 95–152 Pa correspond to critical discharges (Q_c) of 0.2–0.6 m^3 s^{-1} in the LUZ at A_{ref} and 0.07–0.3 m^3 s^{-1} in the HUZ. Using daily discharge data from the South Fork of the Eel River at Leggett as a proxy for the LUZ and Honeydew for the HUZ [*Snyder et al.*, 2003], scaled to station drainage area, Q_c is exceeded on 0.3–2% of all days in the LUZ and 7–19% of all days in the HUZ.

a restricted range of conditions [*Snyder et al.*, 2000]. Equation (6) provides a useful means of characterizing fluvial longitudinal profiles using power law regressions of empirical or model S and A data [*Snyder et al.*, 2000].

[20] The stochastic threshold approach [*Tucker and Bras*, 2000; Tucker, submitted manuscript, 2002] has incision (E) driven by runoff-generating events, using the Poisson rectangular pulse rainfall model of *Eagleson* [1978]. This model parameterizes the climate state using exponential distributions of rainfall intensity (P), storm duration (T_r) and interstorm period (T_b). These variables can be derived from time series of precipitation data. Tucker (submitted manuscript, 2002) added an analytical solution for the model with a threshold shear stress, based on equation (1b), and a characteristic "bankfull" runoff (R_b) event. This formulation represents hydrology in a simple way: it assumes uniform precipitation basinwide, direct Horton overland flow, and no downstream attenuation of flood waves.

[21] The *Tucker and Bras* [2000] formulation gives long-term average incision rate (E) as a power law function of slope (S) and drainage area (A, a proxy for discharge), as in the simple form of the shear stress model (equation (4)). A simplified presentation of the stochastic threshold model (Table 2) (Tucker, submitted manuscript, 2002) expresses the coefficient of erosion in the slope-area function as the product of three factors:

$$E = K_R K_C K_{\tau c} A^m S^n; \qquad (7)$$

K_R, which encompasses the physical parameters (k_e, a, ρ, g, N, and channel width); K_C, which depends on the stochastic climate parameters (P, T_r, T_b and R_b); and $K_{\tau c}$, which is set by the critical shear stress (τ_c) in the form of a critical runoff (R_c). The exponent on drainage area, m equals $3/5a(1 - b)$ (where b is the exponent relating width to discharge), and the slope exponent, n equals $7/10a$, in the formulation used here (equation (3)). As highlighted in Appendix A, the differences between equations (7) and (4) are that (1) K_C represents discharge and runoff processes, instead of k_q from $Q = k_q A^c$ in equations (4) and (2) inclusion of τ_c in the $K_{\tau c}$ term. The threshold term simply modifies the incision rate (E) based on the magnitude of the threshold ($0 \le K_{\tau c} \le 1$), and equals 1 for τ_c equal to 0 (Figure 3b). At steady state ($U = E$), with spatially uniform U, K_R, and K_C, $K_{\tau c}$ is constant along a channel. Therefore the expected concavity index is unchanged from the prediction of equations (5) and (6) ($m/n = \theta$). Because this model uses rainfall data to parameterize climatic forcing directly, the only parameters that cannot easily be constrained from field data are those in equation (1): τ_c, k_e, and a. In section 5, we apply the stochastic threshold model [*Tucker and Bras*, 2000; Tucker, submitted manuscript, 2002] to a set of bedrock streams in northern California [*Snyder et al.*, 2000, 2003], to constrain values of τ_c and k_e for various values of a, by comparing relief in drainage basins with differing rock uplift and incision rates.

5. Model Application to Coastal Streams of the Mendocino Triple Junction Region

5.1. Setting

[22] In several previous studies, we have analyzed extensively a series of 21 small, coastal streams on the northern California coast near the Mendocino triple junction [*Merritts and Vincent*, 1989; *Snyder et al.*, 2000, 2003]. These drainage basins have received much attention because they are all small ($3-20$ km^2), share similar lithology, and most importantly, have differing uplift histories, allowing for a comparative analysis of channel response to tectonic forcing. Late Quaternary rock uplift rates (U) exhibit a well constrained $8\times$ variation along a 120 km coastal transect, with values from $\sim2.5-4$ mm yr^{-1} in the King Range, just south of the Mendocino triple junction, to $\sim0.3-0.5$ mm yr^{-1} in the southern part of the study area [*Merritts and Bull*, 1989; *Merritts*, 1996]. In addition, orographic enhancement of precipitation in the King Range causes a maximum $\sim2\times$ variation in stream discharge in relation to the low uplift zone [*Snyder et al.*, 2003]. Lithology of the study area is heavily fractured (joint spacing <1 m) Cenozoic mudstone and sandstone. Field Schmidt hammer measurements and joint surveys indicate that the rock resistance does not vary significantly within the study area. Channel width does not appear to respond to the uplift rate change in this field area [*Snyder et al.*, 2003]. Finally, *Snyder et al.* [2000] showed evidence that the streams are close to steady state ($U = E$), which means that channel slopes are adjusted to rock uplift rates, allowing for the substitution of U for E in equation (7). Our recent work in the region focused on comparison of digital elevation, field, and hydrological data sets for streams in the King Range high uplift zone (HUZ) to streams in the southern low uplift zone (LUZ [*Snyder et al.*, 2000, 2003]). We found that a simple form of the shear stress model for bedrock channel incision (equation (4)) cannot explain the observed relationship between channel gradient (S, at a given drainage area) and rock uplift rate (U), unless either (1) the value of a in equation (1) is >2.5, which is significantly higher than we would expect for plucking-dominated bedrock incision [*Whipple et al.*, 2000a]; (2) there are significant, unexplained differences in k_e between the HUZ and LUZ (i.e., over and above enhanced orographic precipitation), perhaps related to differences in erosion process or sediment flux [*Snyder et al.*, 2003] (Figure 4); or (3) τ_c importantly influences the S-U relationship. All three remain plausible explanations. However, we demonstrate here that a model incorporating the minimum possible critical threshold (τ_c for initiation of motion for coarse bedload) provides a plausible explanation without appealing to special circumstances.

5.2. Parameters and Methods

[23] To apply the *Tucker and Bras* [2000] model to the California field area, we (1) derived climate parameters from rainfall data, (2) compiled physical parameters from our previous studies, and (3) compared mean channel steepness of HUZ and LUZ streams. As discussed previously by *Snyder et al.* [2000, 2003], average annual precipitation (P_{ma}) and runoff varies significantly between the uplift rate zones. To account for these interbasin orographic rainfall differences, we used hourly precipitation data from two different stations. For both data sets, we followed the methodology of Eagleson and Hawk [*Eagleson*, 1978; *Hawk and Eagleson*, 1992] to calculate representative Poisson pulse model parameters (P, T_r and T_b) from the precipitation time series, using the criteria of *Restrepo-*
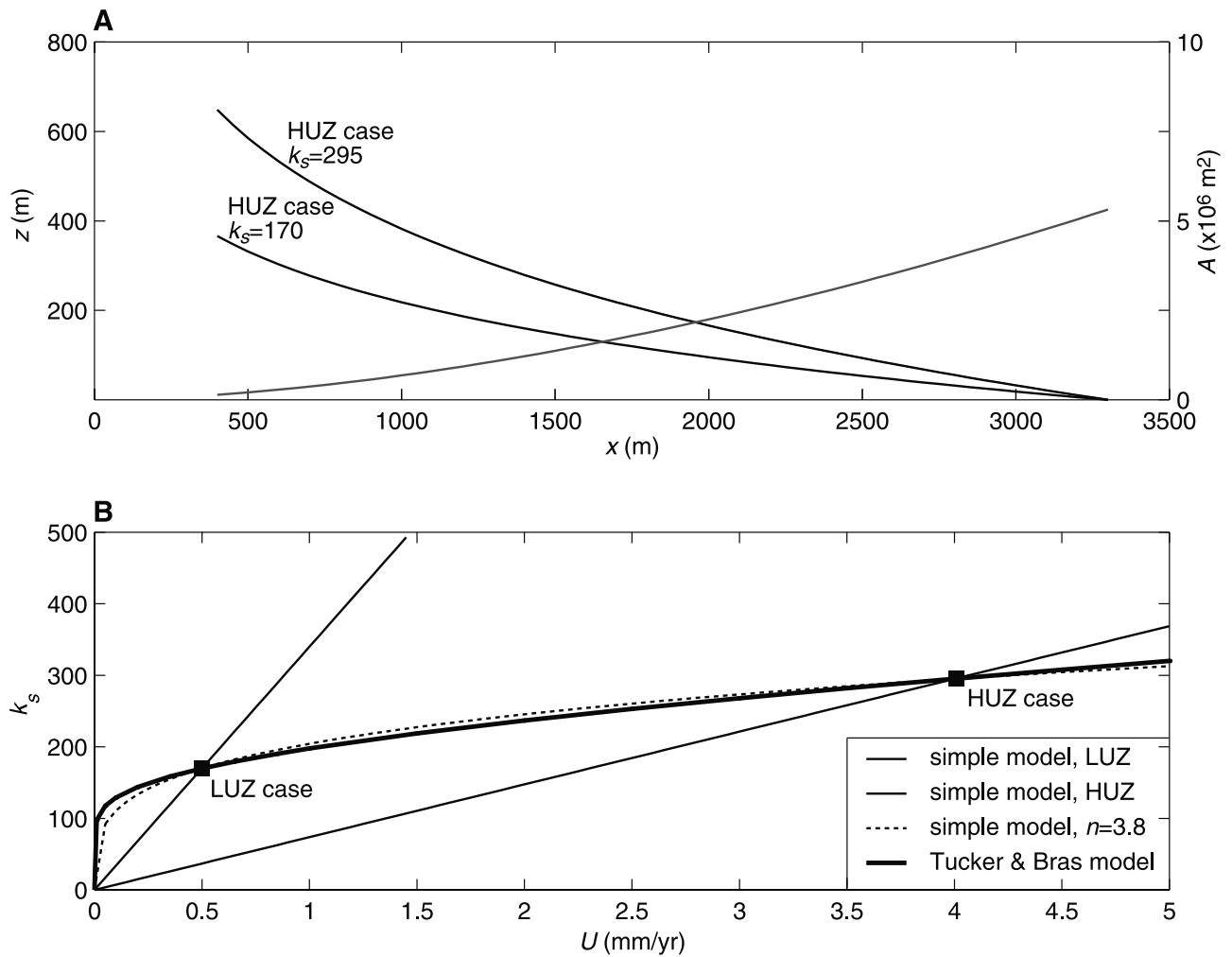
Figure 4. Northern California model setup and results. (a) Model mean steady state high uplift zone (HUZ) and low uplift zone (LUZ) longitudinal profiles (elevation, z versus distance, x; black lines, left axis), used for calculations. Gray line is the drainage area profile (A, right axis). (b) Channel steepness index (k_s, from regressions of S and A; equation (6)) versus uplift rate (U) curves for different shear stress-based incision models, all with slope exponent, $n = 1$, except as noted. Thin, solid lines are the simple form of the shear stress model (equation (4)) with different values of K for the HUZ and LUZ cases [*Snyder et al.*, 2000]. Thin, dashed line is the simple model with constant K, but high slope exponent ($n =$ 3.8) to match both cases [*Snyder et al.*, 2000]. If orographic enhancement of HUZ precipitation is included in this model, then $n \approx 2$ matches both cases [*Snyder et al.*, 2000]. Thick line is the stochastic threshold incision model [*Tucker and Bras*, 2000; Tucker, submitted manuscript, 2002]; see Table 3 for parameters used (the data plotted are for the Eureka climate, with τ_c = 150 Pa). Since channel steepness index (or gradient) is directly related to drainage basin relief, this plot highlights the predictions different incision models make for the relationship between relief and uplift rate. Note particularly that the addition of a threshold term in the model yields a limit on the rate of relief increase with rock uplift rate because erosion becomes more efficient at higher channel gradient as more frequent events exceed the initiation threshold.

Posada and Eagleson [1982] to define independent rainstorms. To represent the low uplift zone, we used a 40-year (1954–1993) record from Eureka, California, just north of the study area. This record had no gaps in data. Unfortunately, no similar record exists for the HUZ. Therefore we used the only two consecutive years (1985–1986) of nearly complete data available for Honeydew, California, to represent the climate state of the HUZ. Honeydew is one of the wettest places in California and is on the east (lee) side of

the King Range (unlike the studied streams, which are the west side), but for reasons explained by *Snyder et al.* [2003], we consider it to be a reasonable proxy for the HUZ climate. The years 1985 and 1986 were somewhat drier than normal, with a mean annual precipitation (P_{ma}) of 1.81 m yr^{-1}, as opposed to 2.66 m yrd^{-1} for 1959 to 1972 (from monthly precipitation data). Furthermore, the data for the Eureka station is measured to 0.01 inch (1 inch = 2.54 cm), while the Honeydew station is precise only to 0.1 inch.

This difference manifests itself predictably in all three of the parameters, increasing mean storm precipitation intensity (P) and duration (T_b), and decreasing mean interstorm period (T_r) for Honeydew (Table 3a). Because the criteria for independent storm events are defined for each individual month, the difference in precision is unimportant in our modeling efforts.

[24] The mean annual precipitation (P_{ma}) predicted by the model ($\langle P \rangle$) can be estimated by multiplying the average storm precipitation intensity (P) by the fraction of time taken up by storm events ($T_r/(T_r + T_b)$). The frequency distributions for rainfall vary seasonally. In the study region, 80–90% of the P_{ma} falls during the half-year period from October to March. To capture this seasonality while retaining a single frequency distribution, we simply average the statistics for the six rainy months and multiply the time fraction by 0.5. This methodology reproduces the true P_{ma} within 6% (Table 3a). The values of $\langle P \rangle$ reflect a roughly 2× increase in precipitation between the LUZ and HUZ, similar to the observed increase in discharge (for a given drainage area) by *Snyder et al.* [2003], suggesting that this parameterization should yield a reasonable approximation of the interbasin orographic effect.

[25] Most of the other necessary model parameters for the HUZ and LUZ were presented in our previous studies [*Snyder et al.*, 2000, 2003] and are reviewed in Table 2. We use data from a representative flood event (17 March 1975 [*Snyder et al.*, 2003]) to parameterize conditions of "bankfull" discharge and width. This event was chosen because it has an ~2 year recurrence interval and exhibits a typical 2× variation in discharge between the HUZ and LUZ. Because the downstream relationship between channel width and drainage area ($w = k'_w A^{b'}$) did not vary demonstrably between the HUZ and LUZ, we use a single parameterization, using high-flow width data (defined by channel morphology, similar to bankfull) in this study [*Tucker and Bras*, 2000; *Snyder et al.*, 2003]. We convert this relationship to width-discharge ($w = k_w Q^b$) using discharge-area data ($Q = k_q A^c$) from the 1975 flood. At-station width measurements for this study area are unavailable, so we use an empirical value from the literature [*Leopold and Maddock*, 1953] for the exponent relating width to discharge at a given channel location ($s = 0.25$). Our calculations assume that infiltration (I) is negligible during storm events, which is consistent with the observed linear relationship between discharge and drainage area during storm events in the region [*Snyder et al.*, 2003]. The calculations presented below are not particularly sensitive to this assumption.

[26] We calculated a range of best fit values of threshold shear stress (τ_c) and shear stress-erosion rate coefficient (k_e) by comparing mean steady state longitudinal profiles from the high uplift zone and low uplift zone (Figure 4a). This gives us two equations (equation (7) for the LUZ and HUZ cases) with which to solve for three unknowns (τ_c, k_e, and a or n). This underdetermination restricts our analysis to finding values of τ_c and k_e for two reference cases, E linear in shear stress ($a = 1$, $n = 0.7$), and E linear in slope ($a = 1.43$; $n = 1$). To demonstrate the influence of orographic precipitation, we did each calculation for two situations: (1) the Eureka/LUZ parameters for both the HUZ and LUZ, and (2) the Eureka parameters for the

LUZ, and the Honeydew/HUZ parameters for the HUZ (Table 3). The implicit assumption that the present-day climate is representative of the past ~100 kyr does not significantly affect our conclusions, just the absolute value of τ_c and k_e, as discussed below. As shown on Table 2, to fully capture the range of acceptable values of τ_c and k_e, we used (1) a maximum range of HUZ channel steepness index (k_s), because this parameter varies significantly amongst the nine streams [*Snyder et al.*, 2000]; and (2) a range of uplift rate estimates, based on approximate uncertainties from the original analyses [*Merritts and Bull*, 1989; *Merritts*, 1996].

5.3. Results and Interpretations

[27] Figure 4b shows that the addition of a critical shear stress and stochastic storms to the bedrock incision model can explain the relationship between channel steepness index (k_s) and uplift rate observed in the Mendocino triple junction region well, without the need to appeal to unexplained changes in k_e or highly nonlinear erosion laws ($a >$ 2.5). As shown in Table 2b, the value of τ_c that best explains the data falls in a narrow range from 95 to 152 Pa (with a maximum range of 45 to 218 Pa) for the various scenarios. The inclusion of orographic enhancement of precipitation has a secondary effect, reducing the necessary value of τ_c by 30–40%. Given the uncertainties (related to temporal and/or spatial changes in climate, tectonics, stream geometry and bed friction), the estimated values of τ_c are imprecise. The important point is heuristic: reasonable values of τ_c can easily account for the otherwise surprisingly low relief contrast between the low uplift and high uplift zones. Thus erosion thresholds cannot be ignored in bedrock channel modeling efforts designed to capture the temporal evolution of landscapes. Moreover, we reiterate that no meaningful value can be assigned to τ_c unless the full stochastic distribution of flood discharges is represented (Figure 3a).

6. Broader Tectonic Implications of the Stochastic Threshold Model

6.1. Relief-Uplift Rate Relationship

[28] As discussed briefly by *Snyder et al.* [2003], the presence of a threshold term fundamentally changes the predicted relationship between steady state channel gradient (and therefore relief) and rock uplift rate. As shown on Figures 4 and 5, when compared to a linear model (equation (4), with $n = 1$), the inclusion of the threshold term reduces the dependence of channel gradient on rock uplift rate, particularly at higher uplift rates: the threshold imparts a nonlinearity that causes minor changes in slope to produce significant changes in erosion rate. This occurs because each incremental change in gradient causes a greater fraction of the stochastic distribution of storm events to initiate incision ($K_{\tau c}$ approaches 1, Figure 3). For lower values of k_e (more resistant rock), the dependence on gradient in response to uplift rates is stronger (Figure 5a). In the northern California study area, the rocks are soft and highly fractured, and therefore the appropriate value of k_e is high and τ_c is low (Table 3 and Figure 4). This likely explains the low relief contrast between the uplift rate zones in the study area. Values of k_e are probably much lower and τ_c much
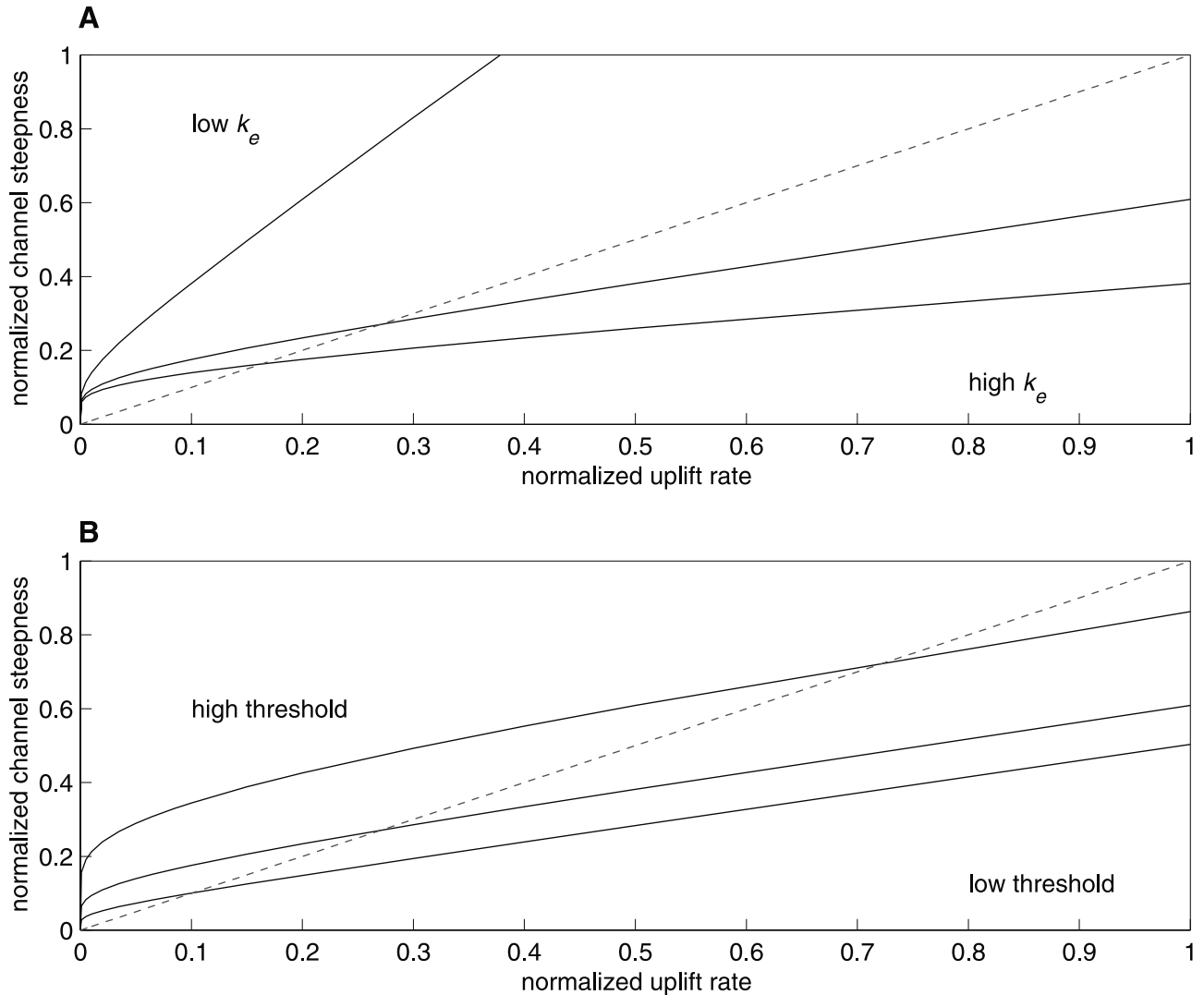
A

B

Figure 5. Predicted relationship between channel steepness index (k_s) and rock uplift rate (U). Solid lines show results for steady state channels using the stochastic threshold model (equation (7)), with $m = 0.51$ and $n = 1$ (Table 3). Dashed lines show the prediction of the simple shear stress model (equation (4)) for steady state channels and $n = 1$ and constant K, for reference. Axes are normalized to highlight general trends. (a) Results for the stochastic threshold model varying the shear stress-incision rate coefficient (k_e). (b) Results for the stochastic threshold model varying the critical shear stress term (τ_c).

higher in areas with more competent, less fractured rock. As demonstrated by Figure 5, this would correspond to greater relief contrasts between uplift rates.

6.2. Predictions for Spatially Variable Rock Uplift Rate

[29] Many streams cross regions of variable rock uplift rates, such as tilting blocks or fault bend fold anticlines. Using a power law for the relationship between U and stream distance (x), *Kirby and Whipple* [2001] derived the predicted channel concavity index for this situation using the simple form of shear stress model (equation (4)). They were able to demonstrate that the concavity index of streams crossing the Siwalik Hills in Nepal was affected by uplift rates in a manner consistent with predictions, and further they were able to calibrate an incision model to make inferences about erosion rates using fluvial topography. Here we extend their analysis to investigate how the

stochastic threshold model (equation (7)) influences streams undergoing spatially variable U (Figure 6). Following Kirby and Whipple, we begin with a power law relationship between U and x:

$$U = k_u x^r, \tag{8a}$$

where k_u is a dimensional constant, and r is an exponent (Figure 6c). Using the empirical, power law relationship between distance and drainage area ($A = k_a x^h$ [*Hack*, 1973]), we obtain

$$U = k_u k_a^{-r/h} A^{r/h}. \tag{8b}$$

The close correspondence between the solutions with the Tucker and Bras model (equation (7)) and the nonlinear
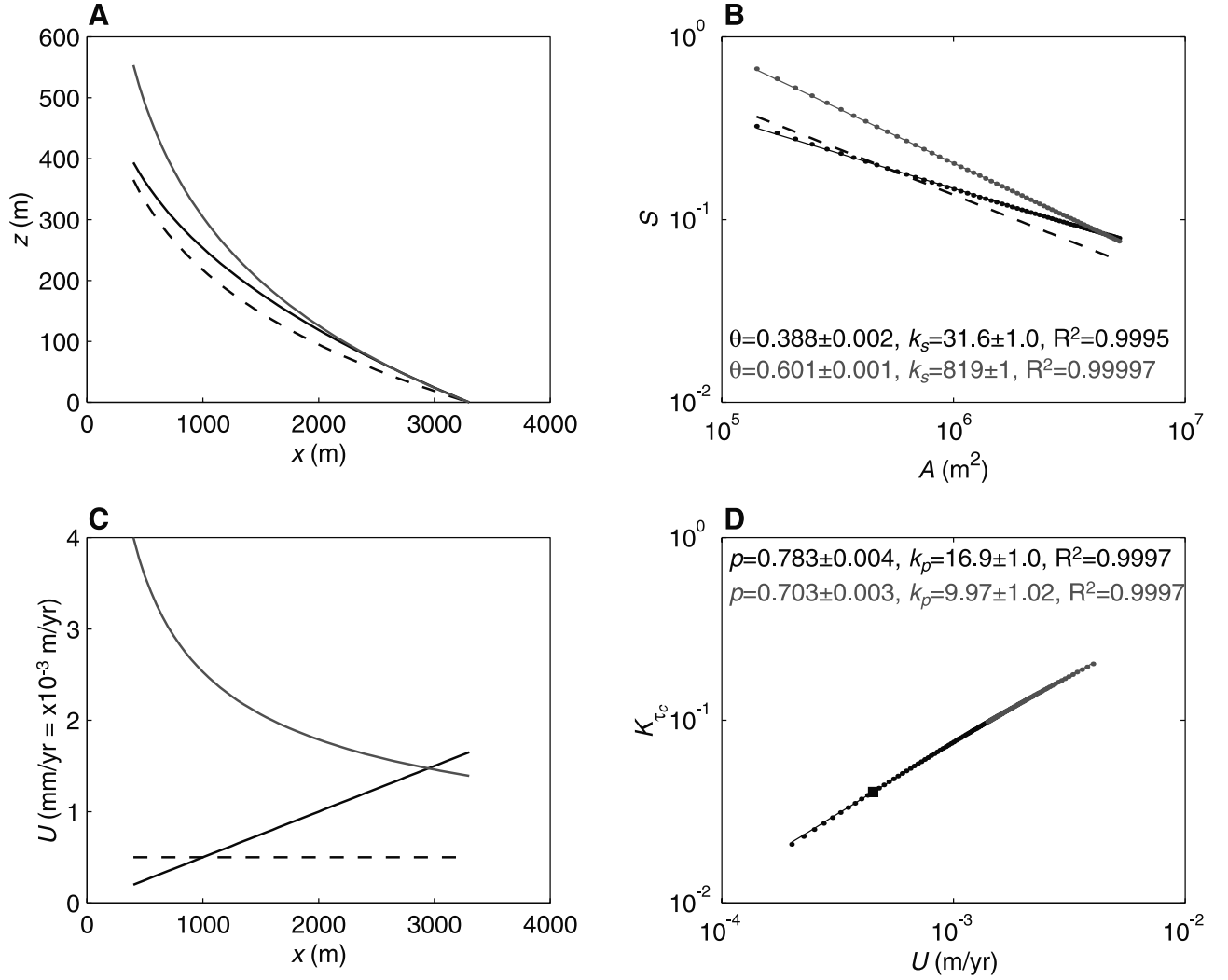
Figure 6. Effect on channel concavity of spatially varying uplift rate (U) using the stochastic threshold model. In all frames, the dashed lines show a case with constant U ($U = 0.0005$ m yr^{-1}), solid lines show a case where $U = U(x)$. For the black line, $U = 5 \times 10^{-7}x$, for the gray line, $U = 0.08x^{-0.5}$. Parameter values for these model runs are the same as those shown on Table 2b for Eureka climate parameters and $n = 1$. (a) Steady state channel longitudinal profiles, elevation (z) against distance (x). Note that the $U(x)$ cases have different concavity. (b) Channel gradient (S)–drainage area (A) power law regressions (equation (6)). The constant U case (dashed line) has $\theta = 0.51 = m/n$ and $k_s = 170$. (c) Uplift rate functions used. (d) $K_{\tau c}$–U power law regressions, using equation (9a). Box indicates the $K_{\tau c}$–U relationship for the constant U case. Note that in the regressions (Figures 6b and 6d) the line (solid) does not perfectly match the data points in the $U(x)$ case due to deviation of the equation (9a) relation from power law form. The difference in the best fit values of p in Figure 6d is solely the result of regression over differing ranges of U. The predicted channel concavity index (Θ, equation (11)) for this these cases is 0.388 and 0.601, respectively, which matches the observed concavity index (θ) closely.

form ($n = 3.8$) of the simple model (equation (4)) on Figure 4b suggests that the relationship between $K_{\tau c}$ and rock uplift rate (U) can be reasonably approximated as a power law:

$$K_{\tau c} \approx k_p U^p, \qquad (9a)$$

where k_p is a dimensional constant and p is a positive exponent. Recall that $K_{\tau c}$ is expected to vary with U because in steeper channels a greater fraction of storms will generate shear stresses in excess of the threshold. The exponent (p) depends on a variety of factors including n,

k_e, τ_c, and P. As seen in Figure 6d, in practice, this relation is only approximate because of the complicated form of the expression for $K_{\tau c}$ (Table 2). Thus p is also a function of the range of uplift rates affecting the channel. As seen in Appendix A, $K_{\tau c}$ depends primarily on the ratio R_c/P, where the critical runoff (R_c) is set by τ_c [*Tucker and Bras*, 2000; Tucker, submitted manuscript, 2002]. Developing the exact theoretical relationship approximated by equation (9a) is unnecessary for this analysis; it is sufficient to note that p varies in concert with k_e and τ_c (specifically τ_c/P, Appendix A (Tucker, submitted manuscript, 2002)).

[30] Next, Substituting equation (8b) into (9a), we obtain

$$K_{\tau c} \approx k_p k_u^p k_a^{-pr/h} A^{pr/h}. \qquad (9b)$$

Equations (8b) and (9b) can then be substituted into equation (7) and solved for channel gradient (S_e) at steady state ($U = E$):

$$S_e \approx \left(\frac{k_u^{1-p}}{k_a^{(1-p)r/h} k_p K_R K_C} \right)^{1/n} A^{[(m/n)-(1-p)(r/hn)]}. \qquad (10)$$

As with equation (5), equation (10) is a similar form to equation (6), suggesting the following equation for predicted channel concavity index (Θ):

$$\Theta \approx (m/n) - (1-p)(r/hn), \qquad (11)$$

which is equivalent to the empirical channel concavity index (θ) in the case where $U(x)$ equals $E(x)$ and K_R and K_C are spatially constant. As shown graphically in Figure 6, this prediction works well for small variations in U. However, if U varies across several orders of magnitude significant departure from the power law form assumed in equation (9) occurs and the actual concavity index drifts from the value predicted by equation (11).

[31] Equation (11) demonstrates how the channel concavity index is affected by spatially variably rock uplift, using the stochastic threshold approach. Using the simple shear stress model (equation (4)), *Kirby and Whipple* [2001] found that the intrinsic concavity index (Θ) was (m/n)-(r/hn). Here the dependence of Θ on the $U(x)$ relation (equation (8a)) is reduced by the factor ($1-p$), which is on the order of 0.25 ($p \approx 0.75$) for typical northern California parameters (Figure 6d). Of course, the value of p is reduced if k_e or τ_c are reduced, diminishing this effect. The stochastic threshold model predicts less effect on channel concavity index by spatially variable U than the simpler model. The effects of a stochastic distribution of floods and an erosion threshold should be considered when interpreting such data in the future.

7. Discussion
7.1. Critical Shear Stress

[32] We have presented two independent estimates of the critical shear stress required to initiate bedrock incision. Both suggest that relatively small thresholds ($\tau_c \approx 100-200$ Pa, 1–2 orders of magnitude less than the shear stress generated by the extreme flood events of *Baker and Kale* [1998] but consistent with the minimum estimates of *Magilligan* [1992]) are appropriate and important for these field sites, although the similarity of the two estimates is probably coincidental. Using a typical Shields threshold of incipient motion for well-sorted sediment [e.g., *Buffington and Montgomery*, 1997], this range of shear stress should correspond to a particle diameter of 10–20 cm. In the case of the Fall Creek analysis, the small τ_c is expected: because the blocks have a small height-to-length ratio, they should be transported relatively easily [*Whipple et al.*, 2000a]. In this situation, plucking is likely a two-stage process. First, joints are expanded, and blocks are loosened and prepared for plucking by weathering processes (wedging of sediment

grains and wood, frost action, etc.). Second, a flood event of sufficiently high shear stress occurs to put the blocks into motion. Because the bedrock at Fall Creek is cut pervasively by open, widely spaced joints, we suspect that the second process is rate limiting.

[33] The low, estimated τ_c values for the California streams merit some discussion. Because these streams are much steeper (S $\gg$ 0.01) than Fall Creek, these shear stresses correspond to high-frequency events. In the high uplift zone, the range of τ_c values (Table 3b) corresponds to discharges that occur $\sim$7–19% of all days (on the order of mean annual discharge), and in the low uplift zone, 0.3–2% of all days (approximate recurrence interval on the order of the 1-year flood). For comparison, discharges equal to or greater than the October 1981 Fall Creek flood have occurred only twice in the 75-year record, corresponding to $\sim$0.007% of the days during the period. The particularly high frequency of erosive events in the HUZ can provide a plausible explanation for the apparent increase in the effectiveness of erosion processes seen in our previous work (i.e., higher K [*Snyder et al.*, 2000]). As mentioned above, this shear stress should mobilize 10–20 cm particles, which approximate the size of the typical sediment produced from the pervasively fractured bedrock (joint spacing 0.01–1 m) and that are observed on the channel beds. This might indicate that the threshold to initiate motion or entrain the bed particles limits incision in the California streams.

[34] Most importantly, the California results indicate that even a threshold small enough to be exceeded annually dramatically changes the predicted relationship between rock uplift rate and channel steepness index, introducing an important additional nonlinearity to the channel incision process that strongly limits the rate of relief increase with rock uplift rate (Figure 4b). This effect is most significant in systems with less resistant rock (high values of k_e and low τ_c), such as the northern California streams with heavily fractured, easily plucked rock; in streams incising harder rocks, we might expect a stronger relationship between channel steepness index and uplift rate (Figure 5a).

7.2. A Nonunique Solution

[35] In recent years, much attention has been paid to the hypothesized role of sediment flux (Q_s) in determining rates of bedrock erosion [e.g., *Howard*, 1980; *Beaumont et al.*, 1992; *Sklar and Dietrich*, 1998]. The approach presented here implicitly assumes that the role of sediment flux in determining erosion rates is encompassed by the inclusion of τ_b and τ_c in the model. *Whipple and Tucker* [2002] present a means to compare generalized versions of several sediment flux models using an approach based on channel gradient and drainage area, as in equation (4). None of these models include an erosion threshold. Several formulations of these models can provide equally plausible explanations for the observed topography in the northern California study area, under a restricted set of conditions that we outline briefly below. First, the present-day low uplift zone (LUZ) channels must be strongly armored by sediment, and therefore approaching a transport-limited condition, meaning that the channel slope is more governed by the need to transport the sediment load than by the stream's intrinsic ability to erode the substrate. Second, the high uplift zone (HUZ) channels must be in a transient condition, with sediment

flux lagging behind channel response. In this situation, as the HUZ streams approach steady state these channels will also become sediment armored and channel gradient will increase, yielding a much stronger relationship between channel gradient and uplift rate at steady state. The sediment protection explanations require that the HUZ channels will physically steepen $4\times$ over the next few hundred kiloyears as sediment flux increases in the HUZ, and the beds of HUZ channels become protected [*Whipple and Tucker*, 2002]. In principle, these models are testable, because in the LUZ, the long-term average sediment flux (Q_s) should approximately equal the carrying capacity (Q_c) if the system is approximately transport limited. At present, the available data [*Snyder et al.*, 2000, 2003] are insufficient to confirm or refute the existence of these conditions in the northern California study area.

[36] Unfortunately, we cannot yet discriminate confidently between the various bedrock channel incision models to explain the northern California relief-uplift rate relationship. To do so would require direct quantitative estimates of long-term sediment flux and average transport capacity that cannot easily be made at present. Regardless of the relative importance of sediment flux, critical shear stress, and other factors such as debris flows [*Stock and Dietrich*, 1998] and intrabasin orographic effects [*Roe et al.*, 2002] to the specific case of the Mendocino triple junction region, the results presented here show that including even minimum values of τ_c and a stochastic distribution of storms yields demonstrably important, first-order effects, that should be included in future models and in the evaluation of field incision rate data. Moreover, such a model provides a sufficient explanation of the Mendocino triple junction region data, based only on processes that we know are occurring. A more complete model will be able to include both these and sediment flux effects.

8. Conclusions

[37] Our work in New York demonstrates the importance of high-magnitude floods in driving incision of bedrock. By using a model that includes both a critical shear stress for incision and a well-constrained stochastic precipitation distribution this observation can be applied to models of fluvial erosion over geologic timescales. Our work in northern California demonstrates that a stochastic threshold model can explain the observed topography without need to appeal to highly nonlinear erosion models ($n > 3$). We find that relatively low erosion thresholds ($\tau_c = 100-200$ Pa) are appropriate for the field settings considered here, and have significant effects on the relationship between relief and rock uplift rate, when compared to models without such a threshold. Therefore efforts to model landscape evolution will be most successful in reproducing the temporal and spatial evolution of topography in active mountain belts if they use a stochastic threshold model.

[38] Although much progress has been made, bedrock river modeling efforts are still hampered by the dearth of field and experimental data to constrain the unknown parameters (equation (1)). Experimental work by *Sklar and Dietrich* [2001] is making important contributions to quantifying rock resistance to erosion in environments dominated by abrasion. Additional studies are needed in

laboratories and field settings of known bedrock incision processes and rates, so that we can constrain the role of sediment flux and values of τ_c, k_e and a for different lithologies and erosion processes [*Whipple et al.*, 2000b]. Also, tests of the incision models in well-parameterized streams that are actively responding to changes in tectonic or climatic forcings must be done. With more work in well-chosen sites, our ability to model the long-term growth and decay of topography will be greatly improved, allowing for more rigorous testing of hypothesized feedbacks among crustal, surficial, and atmospheric processes [e.g., *Molnar and England*, 1990; *Raymo and Ruddiman*, 1992; *Small and Anderson*, 1995; *Whipple et al.*, 1999; *Willet*, 1999]. For instance, only by incorporating realistic representations of flood magnitudes and frequencies, and the physics of the erosion processes, can we begin to make quantitative inferences about the relationship between climatic variability and the efficiency of terrestrial erosion [e.g., *Molnar and England*, 1990; *Bull*, 1991; *Peizhen et al.*, 2001].

Appendix A: Bedrock Channel Incision Models

[40] The basic postulate is

$$E = k_e(\tau_b - \tau_c)^a \text{ or } k_e(\tau_b^a - \tau_c^a),$$

$$E = KA^m S^n,$$

$$K = K_R K_C K_{\tau c}; \ n = \beta a; \ m = \alpha a(1 - b).$$

The basic shear stress model ($\tau_c = 0$) is

$$K_R = k_e k_w^{-\alpha a} k_t^a,$$

$$K_C = k_q^{\alpha(1-b)},$$

$$K_{\tau c} = 1.$$

Empirical relations are as follows:

Physical parameters

$$k_t = \rho g N^\alpha$$

Discharge-drainage area

$$Q = k_q A^c$$

Width-discharge

$$w = k_w Q^b$$

At-station width-discharge

$$w/w_b = (Q/Q_b)^s$$

"Bankfull" discharge-runoff

$$Q_b = R_b A.$$

The stochastic threshold model [*Tucker and Bras*, 2000; Tucker, submitted manuscript, 2002] is

$$K_R = k_e k_w^{-\alpha a} k_t^a,$$

$$K_C = \left(\frac{T_r}{T_r + T_b}\right)^{1-\varepsilon_b} P^{\gamma_b} R_b^{\varepsilon_b} \exp\left(\frac{1}{P}\right) \Gamma(\gamma_b + 1),$$

$$K_{\tau c} = \frac{\Gamma\left(\gamma_b + 1, \frac{R_c}{P}\right) - \left(\frac{R_c}{P}\right)^{\gamma_b} \exp\left(\frac{R_c}{P}\right)}{\Gamma(\gamma + 1)}.$$

The exponents are

$$\alpha = \frac{3}{5}; \beta = \frac{7}{10}$$

for the Manning relation, and

$$\gamma_b = \alpha a (1 - s),$$

$$\varepsilon_b = \alpha a (b - s).$$

References

Baker, V. R., and V. S. Kale, The role of extreme floods in shaping bedrock channels, in *Rivers Over Rock: Fluvial Processes in Bedrock Channels*, *Geophys. Monogr. Ser.*, vol. 107, edited by K. J. Tinkler and E. E. Wohl, pp. 153–165, AGU, Washington, D. C., 1998.

Baldwin, J. A., K. X. Whipple, and G. E. Tucker, Implications of the shear-stress river incision model for the timescale of post-orogenic decay of topography, *J. Geophys.*, *108*, doi:2001JB000550, in press, 2003.

Barnes, H. H., Roughness characteristics of natural channels, *U.S. Geol. Surv. Water Supply Pap.,r 1849*, 213 pp., 1967.

Beaumont, C., P. Fullsack, and J. Hamilton, Erosional control of active compressional orogens, in *Thrust Tectonics*, edited by K. R. McClay, pp. 1–18, Chapman and Hall, New York, 1992.

Benda, L., and T. Dunne, Stochastic forcing of sediment supply to channel networks from landsliding and debris flow, *Water Resour. Res.*, *33*(12), 2849–2863, 1997.

Buffington, J. M., and D. R. Montgomery, A systematic analysis of eight decades of incipient motion studies, with special reference to gravel-bedded rivers, *Water Resour. Res.*, *33*(8), 1993–2029, 1997.

Bull, W. B., *Geomorphic Responses to Climatic Change*, 326 pp., Oxford Univ. Press, New York, 1991.

Coon, W. F., Estimation of roughness coefficients for natural stream channels with vegetated banks, *U.S. Geol. Survey Water Supply Pap.*, *2441*, 133 pp., 1998.

Eagleson, P. S., Climate, soil, and vegetation, 2, The distribution of annual precipitation derived from observed storm frequencies, *Water Resour. Res.*, *14*(5), 713–721, 1978.

Gomez, B., and M. Church, An assessment of bed load sediment transport formulae of gravel bed rivers, *Water Resour. Res.*, *25*(6), 1161–1186, 1989.

Hack, J. T., Studies of longitudinal stream profiles in Virginia and Maryland, *U.S. Geol. Surv. Prof. Pap.*, *294-B*, 42–97, 1957.

Hack, J. T., Stream profile analysis and stream-gradient index, *J. Res. U.S. Geol. Surv.*, *1*(4), 421–429, 1973.

Hancock, G. S., R. S. Anderson, and K. X. Whipple, Beyond power: Bedrock incision process and form, in *Rivers Over Rock: Fluvial Processes in Bedrock Channels*, *Geophys. Monogr. Ser.*, vol. 107, edited by K. J. Tinkler and E. E. Wohl, pp. 35–60, AGU, Washington, D. C., 1998.

Hawk, K. L., and P. S. Eagleson, Climatology of station storm rainfall in the continental United States: Parameters of the Bartlett-Lewis and Poisson rectangular pulses models, Mass. Inst. of Technol., Cambridge, 1992.

Howard, A. D., Thresholds in river regimes, in *Thresholds in Geomorphology*, edited by D. R. Coates and J. D. Vitek, pp. 227–258, Allen and Unwin, Concord, Mass., 1980.

Howard, A. D., Long profile development of bedrock channels: Interaction of weathering, mass wasting, bed erosion, and sediment transport, in

Rivers Over Rock: Fluvial Processes in Bedrock Channels, *Geophys. Monogr. Ser.*, vol. 107, edited by K. J. Tinkler and E. E. Wohl, pp. 297–320, AGU, Washington, D. C., 1998.

Howard, A. D., and G. Kerby, Channel changes in badlands, *Geol. Soc. Am. Bull.*, *94*, 739–752, 1983.

Howard, A. D., M. A. Seidl, and W. E. Dietrich, Modeling fluvial erosion on regional to continental scales, *J. Geophys. Res.*, *99*, 13,971–13,986, 1994.

Kirby, E., and K. X. Whipple, Quantifying differential rock-uplift rates via stream profile analysis, *Geology*, *29*, 415–418, 2001.

Leopold, L. B., and T. Maddock Jr., The hydraulic geometry of stream channels and some physiographic implications, *U.S. Geol. Surv. Prof. Pap.*, *252*, 57 pp., 1953.

Magilligan, F. J., Thresholds and the spatial variability of flood power during extreme floods, *Geomorphology*, *5*, 373–390, 1992.

Merritts, D. J., The Mendocino triple junction: Active faults, episodic coastal emergence, and rapid uplift, *J. Geophys. Res.*, *101*, 6051–6070, 1996.

Merritts, D., and W. B. Bull, Interpreting Quaternary uplift rates at the Mendocino triple junction, northern California, from uplifted marine terraces, *Geology*, *17*, 1020–1024, 1989.

Merritts, D., and K. R. Vincent, Geomorphic response of coastal streams to low, intermediate, and high rates of uplift, Mendocino junction region, northern California, *Geol. Soc. Am. Bull.*, *101*, 1373–1388, 1989.

Molnar, P., and P. England, Late Cenozoic uplift of mountain ranges and global climate change: Chicken or egg?, *Nature*, *346*, 29–34, 1990.

Mullins, H. T., E. J. Hinchey, R. W. Wellner, D. B. Stephens, W. T. Anderson, T. R. Dwyer, and A. C. Hine, Seismic stratigraphy of the Finger Lakes: A continental record of Heinrick event H-1 and Laurentide ice sheet instability, in *Subsurface Geologic Investigations of New York Finger Lakes: Implications for Late Quaternary Deglaciation and Environmental Change*, edited by H. T. Mullins and N. Eyles, *Spec. Pap. Geol. Soc. Am.*, *311*, 1–35, 1996.

Peizhen, Z., P. Molnar, and W. R. Downs, Increased sedimentation rates and grain size 2-4 Myr ago due to the influence of climate change on erosion rates, *Nature*, *410*, 891–897, 2001.

Raymo, M. E., and W. F. Ruddiman, Tectonic forcing of late Cenozoic climate, *Nature*, *359*, 117–122, 1992.

Restrepo-Posada, P. J., and P. S. Eagleson, Identification of independent rainstorms, *J. Hydrol.*, *55*, 303–319, 1982.

Roe, G. H., D. R. Montgomery, and B. Hallet, Effects of orographic precipitation variations on steady-state river profiles and relief, *Geology*, *30*, 143–146, 2002.

Sklar, L., and W. E. Dietrich, River longitudinal profiles and bedrock incision models: Stream power and the influence of sediment supply, in *Rivers Over Rock: Fluvial Processes in Bedrock Channels*, *Geophys. Monogr. Ser.*, vol. 107, edited by K. J. Tinkler and E. E. Wohl, pp. 237–260, AGU, Washington, D. C., 1998.

Sklar, L., and W. E. Dietrich, Relating rates of fluvial bedrock erosion to rock strength: An experimental study (abstract), *Eos Trans. American Geophysical Union*, *80*(46), Fall Meet. Suppl., F448, 1999.

Sklar, L., and W. E. Dietrich, Sediment and rock strength controls on river incision into bedrock, *Geology*, *29*, 1087–1090, 2001.

Small, E. E., and R. S. Anderson, Geomorphically driven Late Cenozoic rock uplift in the Sierra Nevada, *California, Science*, *270*, 277–280, 1995.

Snyder, N. P., K. X. Whipple, G. E. Tucker, and D. J. Merritts, Landscape response to tectonic forcing: DEM analysis of stream profiles in the Mendocino triple junction region, northern California, *Geol. Soc. Am. Bull.*, *112*, 1250–1263, 2000.

Snyder, N. P., K. X. Whipple, G. E. Tucker, and D. J. Merritts, Channel response to tectonic forcing: Analysis of stream morphology and hydrology in the Mendocino triple junction region, northern California, *Geomorphology*, in press, 2003.

Stock, J. D., and W. E. Dietrich, Channel incision by debris flows: A missing erosion law?, *Eos Trans. AGU*, *79*(45), Fall Meet. Suppl., F366, 1998.

Stock, J. D., and D. R. Montgomery, Geologic constraints on bedrock river incision using the stream power law, *J. Geophys. Res.*, *104*, 4983–4993, 1999.

Tinkler, K. J., and E. E. Wohl (Eds.), *Rivers Over Rock: Fluvial Processes in Bedrock Channels*, *Geophys. Monogr. Ser.*, vol. 107, 323 pp., AGU, Washington, D. C., 1998.

Tucker, G. E., and R. L. Bras, A stochastic approach to modeling the role of rainfall variability in drainage basin evolution, *Water Resour. Res.*, *36*(7), 1953–1964, 2000.

Whipple, K. X., and G. E. Tucker, Dynamics of the stream-power river incision model: Implications for the height limits of mountain ranges, landscape response timescales, and research needs, *J. Geophys. Res.*, *104*(B8), 17,661–17,674, 1999.

Whipple, K. X., and G. E. Tucker, Implications of sediment-flux dependent river incision models for landscape evolution, *J. Geophys. Res.*, *107*(B2), 2039, doi:10.1029/2000JB000044, 2002.

Whipple, K. X., E. Kirby, and S. H. Brocklehurst, Geomorphic limits to climate-induced increases in topographic relief, *Nature*, *401*, 39–43, 1999.

Whipple, K. X., R. A. Anderson, and G. S. Hancock, River incision into bedrock: Mechanics and relative efficacy of plucking, abrasion, and cavitation, *Geol. Soc. Am. Bull.*, *112*, 490–503, 2000a.

Whipple, K. X., N. P. Snyder, and K. Dollenmayer, Rates and processes of bedrock incision by the Upper Ukak River since the 1912 Novarupta ash flow in the Valley of Ten Thousand Smokes, *Alaska, Geology*, *28*, 835–838, 2000b.

Willet, S. D., Orogeny and orography: The effects of erosion on the structure of mountain belts, *J. Geophys. Res.*, *104*(B12), 28,957–28,981, 1999.

Willgoose, G., R. L. Bras, and I. Rodriguez-Iturbe, A coupled channel network growth and hillslope evolution model, 1, Theorys, *Water Resour. Res.*, *27*(7), 1671–1684, 1991.

———————————

D. J. Merritts, Geosciences Department, Franklin and Marshall College, Lancaster, PA 17604-3003, USA.

N. P. Snyder, U.S. Geological Survey Pacific Science Center, 1156 High Street, Santa Cruz, CA 95064, USA. (nsnyder@usgs.gov)

G. E. Tucker, School of Geography and the Environment, University of Oxford, Oxford OX1 3TB, UK.

K. X. Whipple, Department of Earth, Atmospheric and Planetary Sciences, Massachusetts Institute of Technology, Cambridge, MA 02139-4307, USA.